JOURNAL OF MATERIALS SCIENCE **40** (2005) 895–901

The control of grain boundary segregation and segregation-induced brittleness in iron by the application of a magnetic field

S. TSUREKAWA*, K. OKAMOTO, K. KAWAHARA, T. WATANABE
Laboratory of Materials Design and Interface Engineering, Department of Nanomechanics, Graduate School of Engineering, Tohoku University, Sendai 980-8579, Japan
E-mail: turekawa@mdie.mech.tohoku.ac.jp

Recycling of iron and steel becomes an universally important issue from the viewpoint of energy and resource saving. Impurity elements like Sn and Cu tend to accumulate in steels by repeated recycling and remarkably degrade mechanical properties of recycled iron alloys due to segregation-induced intergranular embrittlement. The goal of this work is to study the potential of magnetic annealing for the control of grain boundary segregation and intergranular embrittlement in iron alloy. This paper reports several important findings regarding the effect of magnetic annealing on segregation-induced brittleness in iron-tin alloy. Of particular importance is the observations that the concentration of tin at grain boundaries in iron is decreased by magnetic annealing and fracture toughness of iron-tin alloy is drastically improved to the level as high as pure iron.

1. Introduction

It is widely recognized that grain boundary segregation of impurities can exert an influence on a wide variety of materials properties related to cohesion or to kinetics [1]. A number of studies were made of the effects of various impurities in materials [2]. Impurities such as tin, copper and phosphor in iron are often responsible for severe intergranular embrittlement like temper embrittlement [3, 4] and low temperature embrittlement [5, 6]. Seah and Hondros [7] found the empirical correlation of grain boundary enrichment ratios with the inverse solid solubility of the segregant. According to the "Seah–Hondros diagram", these harmful elements in iron have high enrichment factors (more than the value of 10^2), which gives rise to remarkable grain boundary segregation.

Today, recycled materials are universally growing in importance because of savings of material resources, energy and money. In practice, an inevitable accumulation of harmful impurities arising from the service environment and/or the recycling process usually degrades the mechanical properties of recycled materials, largely due to grain boundary segregation. The tin arises from recycled scrap tinplate and copper comes from motors, for example. The concentration of such "tramp elements" in obsolete scrap was predicted to increase to 1.2–1.5 times from the present values [8]. Accordingly, there is a strong demand to find an answer to the problem of this type of degradation in recycling. From the point of view of grain boundary engineering, we may overcome the problem by controlling grain boundary microstructure. Lejcek and Hofman [9] provided the experimental grain boundary segregation diagram (which was first proposed by one of the authors (T.W.) in 1980 [10]), which showed that grain boundary segregation strongly depends on grain boundary character and structure. This type of knowledge suggests that the control of grain boundary microstructure can be used to alleviate segregation-induced embrittlement. If we could produce polycrystalline materials with a high frequency of low energy boundaries that are insensitive to grain boundary segregation, segregation-induced embrittlement would be improved without a reduction of impurity contents.

A new strategy for controlling grain boundary microstructure has been proposed recently. Extensive studies have found that a magnetic field can affect many metallurgical phenomena, particularly grain boundary related phenomena, such as recrystallization [11–14], grain growth [15, 16], phase transformation [17–19], precipitation [20]. Quite recently, we have shown that a magnetic field can suppress tin segregation to grain boundaries in iron [21]. The interesting finding is that segregation-induced embrittlement in polycrystalline materials can be controlled by magnetic annealing. This paper reports further experimental results concerning the beneficial effect of magnetic annealing on grain boundary segregation. Finally, we demonstrate that segregation-induced embrittlement in Fe-Sn alloy can be drastically improved by magnetic annealing.

*Author to whom all correspondence should be addressed.

TABLE I Chemical composition (at.%) of Fe-Sn alloys

Specimen designation	Sn	Si	C	N	P	S	O	Mn
PureFe	–	0.002	0.004	0.002	0,004	0.005	–	0.001
Fe-0.02Sn	0.017	–	0.019	0.008	0.004	0.005	0.15	0.001
Fe-0.2Sn	0.16	–	0.11	0.008	0.004	0.005	0.11	0.001
Fe-0.8Sn	0.80	–	0.12	0.012	0.004	0.005	0.049	0.001

2. Experimental

2.1. Specimen preparation and magnetic annealing

The materials used were Fe-: 0.02, 0.2 and 0.8 at% Sn alloys, which had been prepared by vacuum melting electrolytic iron and high purity tin with 99.999% purity. The chemical composition of these alloys are shown in Table I. The ingot was hot-forged to a plate 10 mm thick and then hot-rolled into 1.2 mm thick sheet at 873 K. Thereafter, specimens of 20 mm × 2 mm × 1 mm in dimensions (suitable for three-point bending fracture test) were cut, mechanically polished and buff-finished to a mirror surface with 3 μm Al_2O_3 particles. Finally, the specimens were electrically polished in a mixture of acetic acid, perchloric acid and methanol with 9:1:1 by volume at 10 V and 1.8 A/cm^2 for FE-SEM/EBPS/OIM measurements.

The samples were subjected to ordinary or magnetic annealing at 973 K ($T/T_c = 0.95$, T_c: The Curie temperature 1023 K) for 6 h in a vacuum of 3×10^{-3} Pa. The magnetic annealing was carried out with magnetic fields of 0.5, 3 and 6 T in a specially designed superconducting magnetic field heating system ($H_{max} =$ 6 T, $T_{max} = 1873$ K) shown in Fig. 1. The direction of the magnetic field was parallel to the rolling direction. The superconducting heat treatment system was composed of a helium free superconducting magnet (Sumitomo Heavy Machine Corporation) and a high-temperature furnace with molybdenum sheet heating element (Futek Furnace inc.). A specially designed carbon sample holder was used for magnetic annealing. Tungsten sheets were inserted between the sample and the carbon holder to avoid carburization of the sample surface due to a contact with the carbon holder.

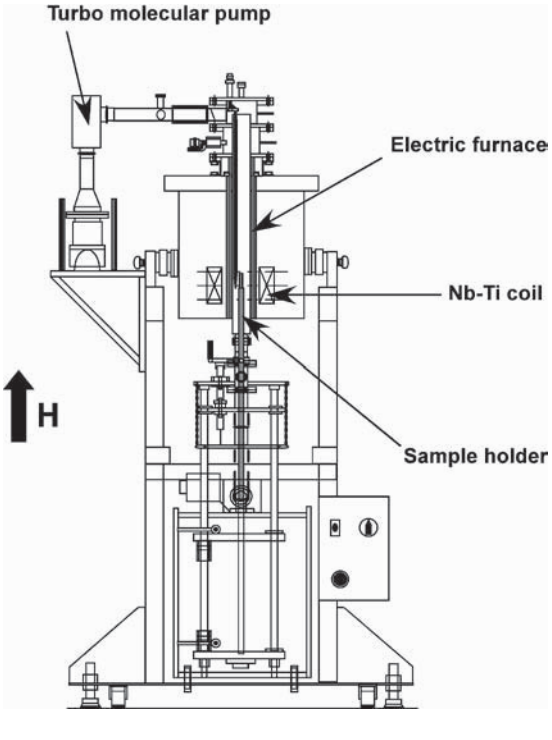

Figure 1 Schematic illustration of superconducting magnetic field heat treatment system.

2.2. Grain boundary microstructure and microchemical analysis

Grain boundary microstructure in magnetically and ordinary annealed samples were examined by orientation imaging microscopy (OIM). The OIM observations were conducted on a Hitachi S-4200 FEG-SEM equipped with TSL OIM system at an accelerating voltage of 30 kV. The electron beam was scanned on the surface using a 3 μm or 6 μm step size.

FEG-TEM/EDS analysis was carried out to examine tin segregation to grain boundaries in magnetically or ordinarily annealed Fe-Sn alloy samples. For TEM/EDS analysis, the annealed samples were mechanically polished to thin sheets of approximately 100 μm thick and then rectangular sheets of 2 mm × 1 mm in dimensions were cut using a wire-saw. Thereafter, the sheets were thinned by a twin-jet technique in a mixture of acetic acid, perchloric acid and methanol with 9:1:1 by volume at 20 V and 0.1 A. Prior to TEM/EDS analysis, the character of individual grain boundaries in the TEM samples were determined by OIM because the grain boundary segregation is well known to depend on the grain boundary character and structure [9, 10, 22]. TEM/EDS analyses were conducted on a Philips FEG-TEM Tecnai F20 or HITACHI FEG-TEM HF-2000 equipped with energy dispersive X-ray spectrometry with an ultra-thin window. For these measurements, the electron beam was converged to approximately 1 nm in diameter. The TEM/EDS analyses were performed 4–7 times along each grain boundary whose character was previously determined by OIM. Such measurements were performed for more than 10 boundaries in each sample annealed at different conditions.

2.3. Grain boundary energy measurement

Atomic force microscopy (AFM) was used to measure the profiles of grain boundary grooves formed during ordinary and magnetic annealing because the grain boundary energy is affected by the amount of impurity/solute segregation [7]. AFM observations were carried out using a SHIMADZU SPM-9500. From the dihedral angle θ obtained, the grain boundary energy was evaluated by,

$$\gamma_{gb} = 2\gamma_s \cos(\theta/2),$$

where γ_{gb} and γ_s are the grain boundary and the surface energies, respectively. For grain boundary energy measurements, the dihedral angles were measured at four different positions along a grain boundary and such

measurements were performed for more than 10 boundaries in each sample. Strictly speaking, the surface energy depends on surface orientation. Nevertheless, the surface energy was assumed to be isotropic in the present study because little reliable information is available from experiments about orientation-dependence of surface energy and actually a facetted surface in a groove profile was not always observed in this study.

2.4. Fracture toughness measurement

The effect of magnetic annealing on segregation-induced embrittlement was studied using three-point bending fracture tests. After magnetic or ordinary annealing, a notch, approximately 150 μm in width and 0.5 mm in length, was introduced into the specimens using a wire saw. The three-point bending tests were conducted at 77 K (in liquid nitrogen) to avoid effect of plastic deformation on fracture, and at a cross-head speed of 0.25 mm/min. The fracture toughness was evaluated as,

$$K_{\mathrm{IC}} = \frac{P}{Wt^{1/2}} Y\left(\frac{a}{t}\right),$$

where P is fracture stress, W the sample width, t the sample thickness and a the notch length, and Y is given by,

$$Y = \frac{S}{W}\frac{3\alpha^{1/2}}{2(1-\alpha)^{3/2}}\left[1.99 - 1.33\alpha - (3.49 - 0.68\alpha + 1.35\alpha^2)\frac{\alpha(1-\alpha)}{(1+\alpha)^2}\right],$$

where $\alpha = (a/t)$ and S is the span length ($S = 12$ mm in this study) [23].

3. Results and discussion

3.1. Grain boundary microstructure

Quantitative analysis of grain boundary microstructures in magnetically and ordinarily annealed Fe-0.02, 0.2 and 0.8 at% Sn alloy samples are tabulated in Table II. The scatter in the average grain sizes in Table II is shown by the standard error. The average grain size tends to decrease with increasing tin content, being 68, 35 and 36 μm for ordinarily annealed Fe-0.02, 0.2 and 0.8 at% Sn alloy samples, respectively. A magnetic field does not have a noticeable effect on the rate of grain growth and the grain boundary character distribution (GBCD) in Fe-Sn alloys irrespective of tin content. The grain boundary character distributions (GBCD) in annealed samples is similar to the theoretically derived distribution for a random polycrystal [24], though the fraction of low angle boundaries was 3–4 times higher in the annealed samples than in random polycrystals. The annealed specimen had a frequency of high energy random boundaries ranging from 78 to 82%, and the total frequency of low angle boundaries and low Σ(3–29) coincidence boundaries was 18–22%.

3.2. Effect of magnetic annealing on grain boundary energy

Fig. 2 shows the grain boundary energy in Fe-0.8at% Sn alloy as a function of the strength of the magnetic field applied during annealing. Although grain boundary energy depends on grain boundary character and structure, we could not determine the character of individual grain boundaries subjected to AFM measurements. The scatter of the data in Fig. 2 may be attributed to differences in grain boundary character and inclination of a grain boundary plane. Of particular importance is the observation that the average values of grain boundary energy increased with increasing magnetic field strength. Seah and Hondros [7], who applied the Gibbs adsorption theorem to grain boundary segregation, demonstrated that the grain boundary energy in Fe-Sn alloys decreases with increasing degree of tin segregation to grain boundaries. Accordingly, the result shown in Fig. 2 suggests that application of a magnetic field can reduce the amount of tin segregation to grain boundaries.

On the other hand, smaller changes in grain boundary energy for Fe-0.02at%, 0.2at% Sn alloys were observed with increasing applied magnetic field strength.

TABLE II Microstructural aspects of ordinarily or magnetically annealed Fe-Sn Alloys

Specimen Designation	Tin concentration (at.%)	Annealing temperature (K)	Magnetic field (T)	Average grain size d(μm)	standard deviation σ(σ/d)	GB character distribution (%)		
						Low Angle	Σ3-Σ29	R
Fe-0.02at.%Sn	0.017	973	0	68 ± 3.6	51 (0.75)	6	12	82
			0.5	72 ± 3.3	45 (0.63)	10	12	78
			3	35 ± 0.7	17 (0.49)	10	11	79
			6	60 ± 2.6	37 (0.62)	7	13	80
Fe-0.2at.%Sn	0.16	973	0	35 ± 0.6	15 (0.43)	8	12	80
			0.5	36 ± 0.7	18 (0.50)	8	10	82
			3	36 ± 0.7	17 (0.47)	10	11	79
			6	32 ± 0.6	15 (0.47)	10	11	79
Fe-0.8at.%Sn	0.80	973	0	36 ± 0.7	17 (0.47)	7	12	81
			0.5	34 ± 0.5	12 (0.35)	9	12	79
			3	35 ± 0.6	15 (0.43)	9	12	79
			6	39 ± 0.9	18 (0.46)	7	11	82

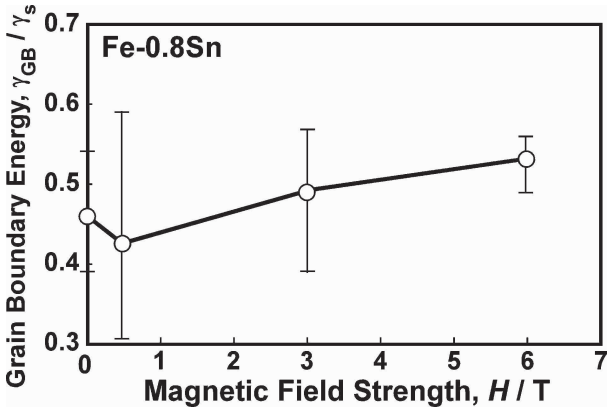

Figure 2 The average relative grain boundary energy in an Fe-0.8 at%Sn alloy as a function of the magnetic field strength applied during annealing.

3.3. Microchemical analysis for grain boundaries by FEG-TEM/EDS

The measurements of tin segregation to grain boundaries were performed by the FEG-TEM/EDS technique. Since grain boundary segregation depends on grain boundary character [9, 10], the OIM analysis was conducted to determine the character of individual boundaries in TEM samples prior to TEM/EDS analysis.

Fig. 3 shows the tin concentration measured along the direction perpendicular to a random grain boundary in the Fe-0.8 at% Sn alloy specimen after ordinary or magnetic ($H = 3$ T) annealing at 973 K for 6 h. We found that grain boundary segregation depends on grain boundary character: the tin concentration was almost 1.5 times higher at the random boundary than in grain interior, while there was no noticeable sign of grain boundary segregation of tin at the low-angle boundary [21]. Surprisingly, TEM/EDS analyses shown in Fig. 3 revealed that the tin concentration at the random boundary decreased down to almost the same value as in the grain interior by magnetic annealing. Therefore, we can confirmed that a magnetic field can reduce the amount of tin segregation to grain boundaries in iron-tin alloy.

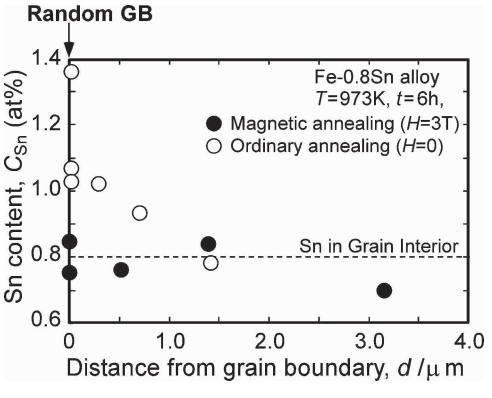

Figure 3 FEG-TEM/EDS analyses showing effect of the magnetic annealing ($T = 973$ K, $t = 6$ h, $H = 3$ T) on tin segregation to random grain boundaries in an Fe-0.8at%Sn alloy. (Note: the magnetic annealing can suppress tin segregation to grain boundaries.)

3.4. The origin of magnetic field effect on grain boundary segregation

3.4.1. Magnetic free energy

The observed beneficial effect of a magnetic field on grain boundary segregation will be discussed from the viewpoint of magnetic free energy. In general, the magnetic free energy in ferromagnetic materials is given for unit volume by,

$$U_f = -\mu_0\left(H - \frac{NM_s}{2}\right)M_s, \tag{1}$$

where μ_0 is the magnetic permeability of vacuum, M_s the saturation magnetization, H the strength of a magnetic field and N the demagnetizing factor. On the other hand, the magnetic free energy in diamagnetic and paramagnetic materials for unit volume is given by,

$$U_d = U_p = -\frac{1}{2}\mu_0\chi(1 - \chi N)H^2 \tag{2}$$

where χ is the susceptibility. If tin atoms, which are in a paramagnetic state at the annealing temperature, segregate to grain boundaries and form "clouds" like another phase, the locally formed "cloud" would influence the magnetic free energy of the system in an applied magnetic field, even though tin atoms do not lower the Curie temperature [25]. The existence of these "clouds" would give rise to an increase in the free energy of the system, because the magnetic free energy may be much higher at the "cloud" than in the grain interior, that is $U_p \gg U_f$, in a high magnetic field. This is because the susceptibility of tin is extremely small (2.7×10^{-8} [26]). From Equations 1 and 2, we estimated the energy difference, $\Delta U = U_f - U_P$, to be approximately -6×10^6 J/m^3 for $H = 6$ T by assuming $N = 0$. According to the temperature dependence of the free energy of grain boundary segregation of tin in iron, which was reported by Seah and Lea [27], the segregation free energy at 973 K is approximately -6.5×10^5J/m^3. Therefore, the magnetic energy is one order of magnitude lower than the grain boundary segregation energy. Consequently, tin atoms can be rejected from the grain boundaries to lower the magnetic free energy of the system when a magnetic field is applied.

On the other hand, it is reasonable to assume that the demagnetizing factor for the "cloud" is much lower when a grain boundary is parallel to the direction of a magnetic field than perpendicular to it, which would yield $U_p(\perp) > U_p(//) \gg U_f$ for a segregant in a paramagnetic state like tin or $U_d(//) > U_d(\perp) \gg U_f$ for segregant in a diamagnetic state like copper. Therefore, it is expected that the effect of a magnetic field on reducing grain boundary segregation of tin is more pronounced when the grain boundary is perpendicular to a magnetic field.

Fig. 4(a) and (b) show the intensity ratio of the peak for tin to iron, I_{Sn}/I_{Fe}, obtained from the EDS measurements at random grain boundaries parallel and perpendicular to the direction of the applied magnetic field during annealing, respectively, as a function of

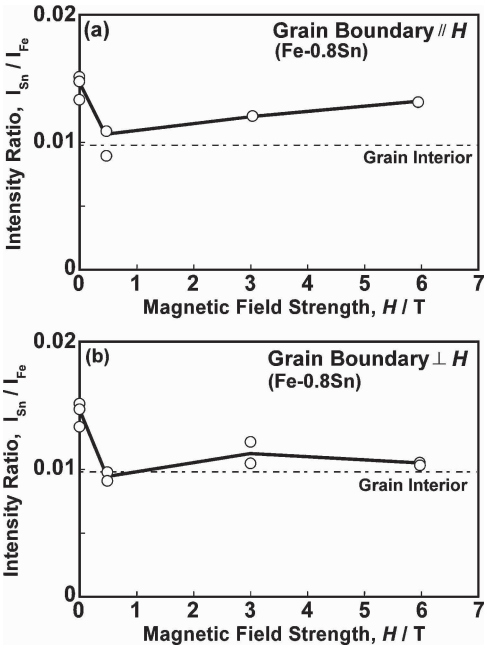

Figure 4 The EDS intensity ratio of the peak for tin to iron at random grain boundaries in an Fe-0.8 at%Sn alloy as a function of the magnetic field strength during annealing: the direction of a magnetic field was (a) parallel and (b) perpendicular to the grain boundary .

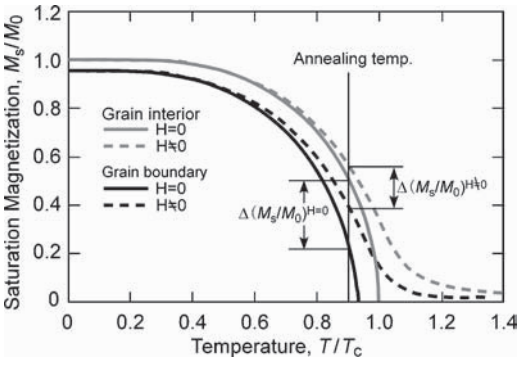

Figure 5 Schematic explanation of a possible mechanism for the observed effect of a magnetic field on grain boundary segregation.

magnetic field strength. Only a slight difference in the effect of magnetic field on grain boundary segregation is seen depending on the direction of a magnetic field. The intensity ratio I_{Sn}/I_{Fe} is found to decrease down to the same level as the grain interior by application of a magnetic field of no more than 0.5 T at random boundaries perpendicular to the direction of a magnetic field. For the grain boundaries parallel to a magnetic field, the intensity ratio was decreased by the application of the magnetic field as well. Nevertheless, the level of the intensity ratio was approximately 1.25 times higher at grain boundaries than in the grain interior. As discussed above, therefore, the suppression of grain boundary segregation of tin (in the paramagnetic state) by magnetic annealing seems to be somewhat more effective when a grain boundary is perpendicular to a magnetic field.

3.4.2. Grain boundary magnetism

There is another possible explanation for the effect of a magnetic field on grain boundary segregation. Szklarz and Wayman [25] and Ishida *et al*. [28], who examined the effect of ferromagnetism on grain boundary segregation, reported that the magnetic transition from paramagnetic to ferromagnetic states induces additional segregation. As for the magnetic property of grain boundary, Szpunar *et al*. [29], who used an amorphous structure in nickel as a model for a random boundary, reported that the magnetic moment increased when the average nearest-neighbor distance approached the value of the fcc structure. On the other hand, Sob *et al*. [30] demonstrated that the magnetic moment in iron was higher at Σ5 boundary than in the grain interior, which agreed with the experimentally observed magnetic moment of a grain boundary in nickel [31, 32], and that the magnetic moment increased with decreasing atomic density. Nevertheless, it is possible that the moment at a grain boundary is lower than in the grain interior due to the presence of impurity atoms like tin [33]. Hence, we assume that the magnetization and Curie temperature of a random boundary decorated with impurities are lower than those of the grain interior, and the difference in the magnetization between the grain interior and the grain boundary at an annealing temperature near the bulk Curie temperature would intensify the grain boundary segregation of tin. In the presence of an external magnetic field, the field-induced magnetization occurs [19] as schematically shown in Fig. 5 [21]. In this case, the difference in the magnetization between grain boundary and grain interior, which can give rise to extra grain boundary segregation due to the magnetic effect, is decreased. Consequently the concentration of tin atoms at a random boundary can decrease in a magnetically annealed sample compared with an ordinarily annealed one.

3.5. Control of segregation-induced embrittlement by application of magnetic field

As shown in the previous section, we have found that the magnetic annealing is useful for controlling harmful segregation of tin to grain boundaries in iron. In this section, we examine whether the segregation-induced intergranular brittleness in iron–tin alloys can be improved by application of a magnetic field. The fracture toughness in iron-tin alloys measured at 77 K is shown in Fig. 6 as a function of magnetic field strength applied during annealing. For comparison, the fracture toughness of pure iron with different grain sizes were shown by the arrows on the vertical axis of right hand side of Fig. 6, which was estimated from the grain size dependence of fracture toughness of pure iron by assuming that the Hall—Petch relation is valid for fracture toughness. Also, the grain sizes shown in Fig. 6 for each alloy are the average values obtained from differently annealed samples. It is worth noting that fracture toughness of iron-tin alloys increases with increasing magnetic field strength irrespective of tin concentration. Surprisingly, the values of fracture toughness became higher for magnetically annealed samples than for pure iron in the range of applied magnetic field strength beyond 3 T. The improvement in brittleness by

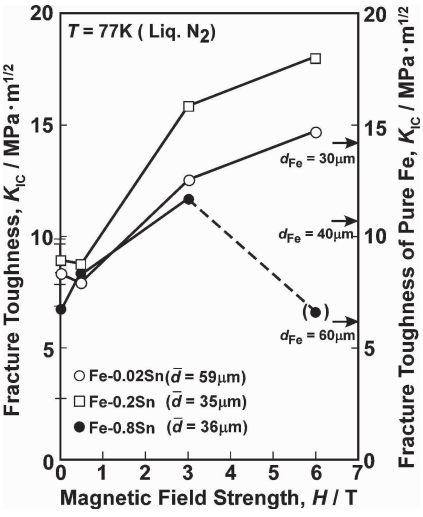

Figure 6 Fracture toughness measured at 77 K for Fe-Sn alloys annealed at 973 K for 6 h with a magnetic field of different strength. For comparison, the fracture toughness of pure iron with different grain sizes are indicated by the arrows along the vertical axis of right hand side. (Note: Fracture toughness of Fe-Sn alloys increases with increasing applied magnetic field strength during annealing. Segregation-induced brittleness can be improved by the magnetic annealing.)

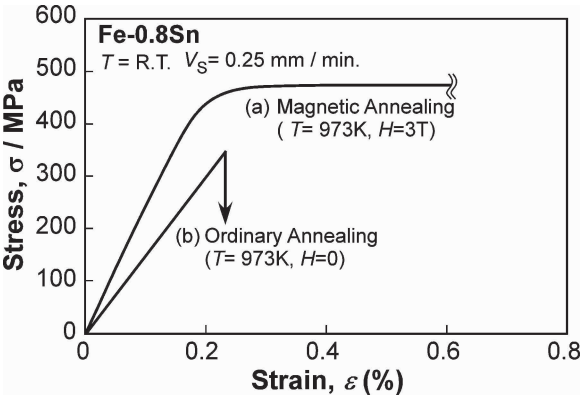

Figure 7 Stress—strain curves obtained from three-point bending tests at room temperature for the Fe-0.8 at%Sn alloy samples annealed at 973 K for 6 h (a) with the 6 T magnetic field and (b) without a magnetic field.

magnetic annealing appeared to be more pronounced in Fe-0.2at%Sn alloy. Generally speaking, fracture toughness can depend on the grain size and the GBCD [34, 35]. Since there were no significant differences in the grain size and the GBCD in annealed iron-tin alloys irrespective of whether a magnetic field was applied, the enhanced fracture toughness in magnetically annealed samples must be achieved as a result of reducing grain boundary segregation of tin by a magnetic field. Fracture toughness of Fe-0.8 at%Sn alloy annealed with a 6 T magnetic field decreased as does the corresponding tin concentration at random grain boundaries (Fig. 4). We have often observed that the largest effect of a magnetic field on grain boundary related phenomena (i.e., sintering of iron powder compact for example [36]) occurs at an optimal field strength. However, the reason has not yet been understood.

From the observations of crack propagation, intergranular fracture predominately occurred at 77 K in iron-tin alloys even after magnetic annealing, while both intergranular and transgranular (cleavage) fracture took place in pure iron. In bcc alloys, solid-solution softening occurs at low-temperatures owing to the aid of the strain field of solute atoms in kink-pair formation on dislocation [37]. The solute-softening effect may be responsible for suppression of cleavage fracture in magnetically annealed iron-tin alloy. The enhanced fracture toughness in iron-tin alloys is therefore probably the result of a combination of the effects of reducing tin concentration at grain boundaries by application of magnetic field and the solid-solution softening.

Finally, the usefulness of magnetic annealing for improving segregation-induced embrittlement was demonstrated clearly. Fig. 7 shows stress—strain curves obtained from 3-point bending tests at room temperature for ordinarily and magnetically ($H = 3$ T) annealed Fe-0.8 at% Sn alloy samples. The ordinarily annealed sample could fracture without plastic deformation even at room temperature. On the other hand, the stress—strain curve for the magnetically ($H = 3$ T) annealed sample obviously showed considerable plastic deformation. Unfortunately, the 3-point bending test for the magnetically annealed sample was interpreted at the strain of approximately 0.6% due to the limitation of the testing jig. From these results, we confirmed that magnetic annealing is useful for achieving enhanced ductility of segregation-induced brittleness in iron-tin alloys.

4. Conclusions

Magnetic annealing was applied to control grain boundary segregation and segregation-induced brittleness in iron-tin alloys. The main results obtained from this work are the following:

(1) The gain boundary energy in the iron-tin alloys increased with increasing applied magnetic field strength during annealing.

(2) FE-TEM/EDS analyses revealed that the tin concentration at random boundaries was decreased by magnetic annealing for the iron-tin alloys. The beneficial effect of the magnetic field on the suppression of tin segregation to grain boundaries was more pronounced when a grain boundary was perpendicular to the magnetic field direction.

(3) The fracture toughness of iron-tin alloys increased with increasing magnetic field strength applied during annealing. The values of fracture toughness became higher in iron-tin alloys than in pure iron for magnetic field strengths beyond 3 T.

(4) Magnetic annealing can be a powerful tool for controlling grain boundary segregation and segregation-induced brittleness in iron alloys.

Acknowledgement

The authors would like to express their hearty thanks to Prof. M. Sob and Prof. R. Faulkner for useful discussion. This work was supported by a Grant-in-Aid for Basic Research (A) (15201015) and COE Research from the Ministry of Education, Science, Sports and Culture of Japan.

References

1. E. D. HONDROS, *Phil. Trans. R. Soc. Lond.* A **295** (1980) 9.
2. W. C. JOHNSON and J. M. BLAKELY (eds.) "Interfacial Segregation," (American Society for Metals, 1979).
3. R. WISWANATHAN, *Scripta Metall.* **8** (1974) 1225.
4. C. J. MCMAHON JR., *Mater. Charact.* **26** (1991) 269.
5. H. R. TIPLER and D. MCLEAN, *J. Metal Sci.* **4** (1970) 103.
6. A. KUMER and B. L. EYRE, *Proc. R. Soc. Lond.* **A370** (1980) 431.
7. M. P. SEAH and E. D. HONDROS, *Proc. Roy. Soc.* **A335** (1973) 191.
8. K. NORO, M. TAKEUCHI and Y. MIZUKAMI, *ISIJ Intern.* **37** (1997) 198.
9. P. LEJCEK and S. HOFMANN, *Interface Sci.* **1** (1993) 161.
10. T. WATANABE, S. KITAMURA and S. KARASHIMA, *Acta Metall.* **28** (1980) 455.
11. R. SMOLUCHOWSKI and R. W. TURNER, *J. Appl. Phys.* **20** (1949) 745.
12. H. O. MARTIKAINEN and V. K. LINDROOS, *Scandinavian J. Metallurgy* **10** (1981) 3.
13. T. WATANABE, Y. SUZUKI, S. TANII and H. OIKAWA, *Phi. Mag. Lett.* **62** (1990) 9.
14. N. MASAHASHI, M. MATSUO and K. WATANABE, *J. Mater. Res.* **13** (1998) 457.
15. T. WATANABE, in "Proc The Fourth Intern. Conf. on Recrystallization and Related Phenomena" (The Japan Inst. Metals, 1999) p. 99.
16. K. HARADA, S. TSUREKAWA, T. WATANABE and G. PALUMBO, *Scripta Mater.* **49** (2003) 367.
17. H. PENDER and R. L. JONES, *Phys. Rev.* **1** (1913) 259.
18. M. SHIMOTOMAI and K. MARUTA, *ibid.* **42** (2000) 499.
19. J.-K. CHOI, H. OHTSUKA, Y. XU and W.-Y. CHOO, *ibid.* **43** (2000) 221.
20. G. SAUTHOFF and W. PITSCH, *Phil. Mag. B* **56** (1987) 471.
21. S. TSUREKAWA, K. KAWAHARA, K. OKAMOTO, T. WATANABE and R. FAULKNER, *Mater. Sci. Eng.* A **387–389** (2005) 442.
22. P. LEJCEK and S. HOFMANN, *Crit. Rev. Sol. State Mater. Sci.* **20** (1995) 1.
23. ASTM Standard E-399-81, "Annual Book of ASTM Standard," Part 10 (1981).
24. A. MORAWIEC, J. A. SZPUNAR and D. C. HINZ, *Acta Metall.* **41** (1993) 2825.
25. K. E. SZKLARZ and M. L. WAYMAN, *ibid.* **29** (1981) 341.
26. K. HONDA, "Magnetic Properties of Matter" (Syokwabo and Company, Tokyo, Japan, 1928) p. 129.
27. M. P. SEAH and C. LEA, *Phil. Mag.* **31** (1975) 627.
28. K. ISHIDA, S. YOKOYAMA and T. NISHIZAWA, *Acta Metall.* **33** (1985) 255.
29. B. SZPUNAR, U. ERB, K. T. AUST, G. PALUMBO and L. J. LEWIS, *Mat. Res. Soc. Symp. Proc*. **318** (1994) 477.
30. M. SOB, I. TUREK, L. WANG and V. VITEK, in Proc. 10th Intern. Metallurgical and Materials Conference, METAL 2001 (TANGER, Ostraba, 2001) p. 1 (CD-ROM).
31. M. R. FITZSIMMONS, A. RÖLL, E. BURKEL, K. E. SIKAFUS, M. A. NASTASI, G. S. SMITH and R. PYNN, *J. Appl. Phys*. **76** (1994) 6295.
32. *Idem*., *NanoStructured Mater*. **6** (1995) 539.
33. M. SOB, Private communication.
34. L. C. LIM and T. WATANABE, *Scripta Metall.* **23** (1989) 489.
35. *Idem.*, *Acta Metall. Mater.* **38** (1990) 2507.
36. S. TSUREKAWA and T. WATANABE, *Mater. Sci. Forum*, **426–432** (2003) 3819.
37. J. W. MITCHELL and P. L. RAFFO, *Can. J. Phys.* **45** (1967) 1047.